



Assessment of the diabetic foot using spiral computed tomography imaging and plantar pressure measurements: A technical report

Kirk E. Smith, AAS; Paul K. Commean, BEE; Michael J. Mueller, PhD, PT; Douglas D. Robertson, MD, PhD; Thomas Pilgram, PhD; Jeffrey Johnson, MD

The Mallinckrodt Institute of Radiology; the Program of Physical Therapy; and the Department of Orthopaedic Surgery at the Washington University School of Medicine, St. Louis, MO 63110

Abstract—Persons with diabetes mellitus (DM) and peripheral neuropathy are at high risk for skin breakdown due to unnoticed excessive pressures to the plantar foot during walking. We developed methods that combined spiral x-ray computed tomography (SXCT) imaging and plantar pressure analysis to quantify internal foot structure and external pressure during plantar loading. Methods were tested using a subject with DM who had a plantar ulcer, and a healthy control. SXCT measurements were within 2 mm of truth and SXCT plantar recordings were within 6.5% of walking trials. Hammer toe deformity (second toe), severe atrophy of the intrinsic muscles and less contact area during plantar loading, and a peak plantar pressure three times greater at the site of the ulcer were measured in the diabetic foot as compared with the healthy control. This preliminary investigation suggests that these methods are accurate for structural and pressure measurements of diabetic and healthy feet.

Key words: *diabetes, foot structure, peripheral neuropathy, plantar pressure, plantar ulcer, spiral computed tomography.*

INTRODUCTION

Patients with diabetes mellitus (DM) and peripheral neuropathy are at high risk for developing neuropathic ulcers on the plantar surface of their feet. Foot disease is

the most common complication of DM leading to hospitalization (1). If infected, these ulcerations can lead to amputation (2). Approximately half of the 50,000 nontraumatic lower limb amputations a year occur in persons with DM (3). The American Diabetes Association estimates that up to 85 percent of these amputations can be prevented (4). The emphasis of the programs to prevent lower limb amputation has been on protection of the “at risk” foot (2,5). In *Healthy People 2000*, the Federal government has set an objective [17.10] to reduce the number of lower limb amputations from 8.2 to 4.9 per 1000 people with DM. Each major amputation that is prevented can save approximately \$63,000 (6), not to mention the savings in morbidity and mortality.

Many factors contribute to skin breakdown on the diabetic foot, but the primary etiology at this time is believed to be excessive, repeated, localized pressure on the insensitive foot (7–9). Theoretically, footwear should be able to protect the insensitive foot from trauma and skin breakdown, but in reality, this often is not the case. There have been no major changes in footwear design since the seminal efforts of Drs. Bauman and Brand in the 1960s (10). These authors emphasized the important principles of distribution of high pressures and using a rigid rocker-bottom sole to reduce forefoot pressures during late stance. Despite studies to verify the benefits of these design principles (11–15), little has been done to advance the state of the art in orthotic design and fabrication. Unfortunately, current orthotic device fabrication is largely an art that depends on the skill and experience of the pedorthist or orthotist.

This material is based in part on work supported by NCMRR, National Institutes of Health.

Address all correspondence and requests for reprints to: Kirk E. Smith, Mallinckrodt Institute of Radiology, 510 S. Kingshighway Blvd. Box 8131, St. Louis, MO 63110; Web: <http://www.mir.wustl.edu/>, <http://medicine.wustl.edu/~muellerm>; email: smithki@mir.wustl.edu.

Most neuropathic ulcers occur under the metatarsal heads (8,16,17). There are several reasons for this, but the two primary reasons appear to be forefoot structural deformity and high pressures during the late stance phase of walking (8,9). In a study of persons with DM attending a metabolic clinic, Holewski et al. (18) report that the prevalence of hammer toe deformity showed the most significant correlation with ulcer/amputation of all factors studied ($p < 0.0001$). Presumably, hammer toe deformity is a complication of peripheral neuropathy. Motor neuropathy causes weakness in the intrinsic muscles of the foot leading to an imbalance between the intrinsic and extrinsic muscles controlling the toes. This imbalance is believed to result in hyperextension of the metatarsal phalangeal joint and distal migration of the metatarsal fat pad. These changes all contribute to making the metatarsal head more prominent and increasing pressures in this area. Gooding et al. have documented a reduction in the soft tissue under the metatarsal heads of subjects with DM compared with healthy controls as measured by high resolution ultrasound (19). Although there is some evidence, the relationship between neuropathy and foot deformity is speculative.

Cavanagh et al. investigated the relationship between static foot structure and plantar pressures during walking for a group of healthy individuals (20). This study investigated the relationship between plantar pressures during walking and standard weight-bearing two-dimensional (2D) radiographs and found that approximately 35 percent of the variance of pressures during walking could be accounted for by measures of foot structure (soft tissue thickness and arch height). Diabetic feet were not studied and, due to the 2D nature of radiographs, the variables studied were limited.

Another study, performed in our lab, investigated the relationship of foot deformity to ulcer location (21). Using clinical measures of foot deformity, we saw a significant relationship between structural deformities and location of skin breakdown.

The study of foot structure and plantar pressure relationships is hampered by the lack of three-dimensional (3-D) structural information of the foot to relate to plantar pressure measurements. There are only a few modalities capable of obtaining 3-D comprehensive sub-surface information; x-ray-computed tomography, magnetic resonance imaging, and ultrasound are the most common. Spiral x-ray CT (SXCT) scanning allows rapid continuous scanning of the limbs and has already replaced conventional CT in many musculoskeletal applications (22). MRI is not feasible for most foot/orthosis scanning due to high cost

and slower rate of data acquisition. MRI also does not allow direct physical density assessment nor does it contain information on cortical bone (where MR signal void is present). Ultrasound is unacceptable due to shadowing by bone and does not effectively penetrate interfaces where an air gap is present. Conventional and digital radiography are projection techniques that involve the loss of 3-D information, introduce geometric distortion, and have relatively poor soft tissue contrast in comparison with spiral x-ray CT. Optical surface methods are effective for capturing foot surface geometry, but provide no subsurface information.

Despite improvements in functional limitations and reductions in peak plantar pressures using treatment with therapeutic footwear, subjects with DM still have substantial deficits in functional limitations and risk for skin breakdown compared with age-matched controls (12,13). A new line of investigation for the design and fabrication of orthotic devices is needed to understand better the mechanisms of injury and how this injury can be prevented. This study presents a way to look "inside the foot" to quantify foot structure in a very accurate and reliable fashion, and relate the structural changes seen in DM and peripheral neuropathy with plantar pressures and ulcers. First, we present a preliminary accuracy assessment of spiral x-ray computed tomography foot measurements, using a healthy volunteer, and compare the results with our previous studies of the lower residual limb. Second, we tested the ability to apply known plantar loads and record the contact area and pressure distribution while in the SXCT scanner. Third, we test and evaluate these methods for quantification of foot structure and plantar pressure for a healthy subject and a subject with DM with peripheral neuropathy and a plantar ulcer.

METHODS

Subjects

We recruited a healthy 40-year-old Caucasian male subject and a 65-year-old Caucasian male subject with DM, peripheral neuropathy, neuroarthropathic deformity of the midfoot, resection of the second metatarsophalangeal joint, and a plantar ulcer at his second metatarsal head. The procedures were explained and informed consent was obtained according to an Institutional Review Board (IRB) approved protocol. These subjects were matched according to weight (83.9 kg), height (1.83 m), and shoe size (11D).

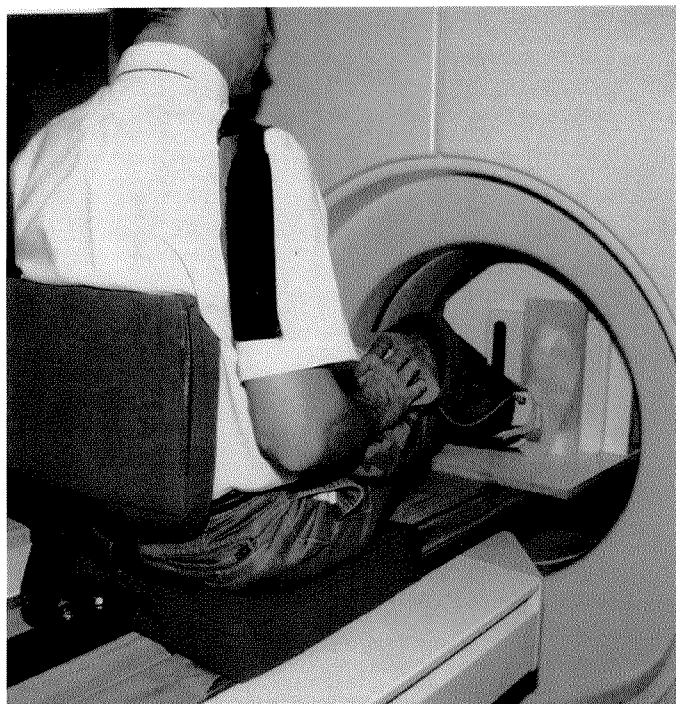


Figure 1.

The custom loading device was used in the SXCT scanner to scan a healthy subject with zero percent and 50 percent of body weight to assess the relationship of plantar pressure to foot structure. Concurrent pressure data was collected. Loads were applied with the foot in 15° of plantar flexion. A digital scale was used to monitor the applied loading conditions.

Equipment

Spiral X-ray Computed Tomography

SXCT scans were collected using a Siemens Somatom Plus S^A in a local hospital. The spiral scanner (23–26) is practical and advantageous (24,27,28) due to improved image quality, minimal x-ray dose, and relatively low cost when compared with other methods for volumetric imaging, especially magnetic resonance methods. SXCT scanning of the limbs avoids exposure of reproductive organs and is considered a low-risk noninvasive technique. We previously validated the SXCT data and image measurement methods on persons with transtibial amputation in our prosthetic fitting system project (29–35). These methods, however, must be validated in the foot, as its structure is quite different from the residual limb.

^A Siemens Medical Systems, Inc., Iselin, NJ

^B Software v. 3.42, Tekscan, Boston, MA

Plantar Pressure Assessment

Plantar pressures were collected using the F-Scan system^B. The system consists of an 0.18-mm thick sensor with 960 pressure-sensing locations. The F-Scan has excellent resolution (each sensel is 0.258 cm²) and thin sensors that did not interfere with SXCT data acquisition. The F-scan system provides reliable measures of relative pressure values. We have extensive experience with this measurement system and have established its reliability in similar conditions (13,36).

Plantar Loading Device

A prototype loading device was designed and built to facilitate an SXCT study of the relationship between foot structure and plantar pressure under static loading conditions (**Figure 1**). The prototype design allows application of loads up to the full body weight of the subject. The apparatus is adjustable to accommodate subjects from 142 to 193 cm in height. The subject pushes against a rigid vertical board with the forefoot while monitoring a strain gage–based scale providing visual feedback of the applied load.

Data Collection

Trials for Subjects with and without Diabetes

The methods were first tested on the healthy subject according to the following protocol. Lead markers were secured at six anatomical locations on the skin surface as follows: 1) distal hallux; 2) posterior calcaneus; 3) lateral aspect of the fifth metatarsal head; 4) medial aspect of the first metatarsal head; 5) dorsal surface of the third metatarsal head; and 6) plantar surface of the midfoot at the arch. Using these markers, a total of 15 caliper measurements were made. A pressure sensor was trimmed to match the volunteers right foot and was taped to the plantar surface with surgical tape. Three 1.5-mm self-adhesive lead markers were attached directly to the sensor at areas that were not being evaluated for pressure, to locate pressure data with SXCT data. The sites used were the center of the plantar surface of the great toe, under the fifth metatarsal head, and plantarly at the center of the heel. A thin nylon stocking was placed over the subject's foot to help secure the sensor. Calibration was performed using full body weight (83.9 kg) and single-legged stance as described by Mueller and Strube (36). A walking trial was performed and data recorded at 50 Hz. The sampling interval having the peak pressure was identified and printed to hardcopy for use as a reference during the SXCT trials.

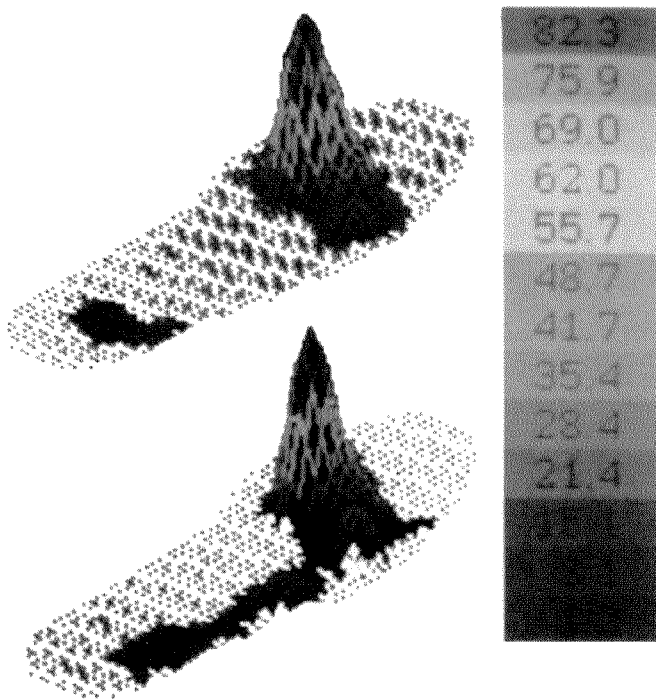


Figure 2.

A trial was conducted to assess the reproducibility of plantar pressure in the SXCT loading device as compared with plantar pressure, which occurs at 80% of stance during walking trials. The F-Scan in-shoe pressure sensor was used and similar pressure distribution and contact area were shown for walking trials (top) and SXCT loading trials (bottom).

CT Scanning

The volunteer was seated in the loading device situated on the SXCT scanner table (**Figure 1**). Historically, late stance phase was believed to be the time period when the forefoot (under metatarsal heads) experienced the highest forces and the lowest contact area resulting in the highest peak plantar pressures (8). We also tested peak plantar pressure during walking and attempted to simulate that instant during stance phase when peak pressures were greatest at the forefoot (**Figure 2**). Therefore, we simulated 80 percent of stance phase during foot loading and concurrent CT scanning. Two scans were acquired in a Siemens Plus S scanner with loading as follows: 1) no load and 2) 50 percent of body weight. A scale with digital readout was monitored by the subject for visual confirmation of applied loads. A display of the peak pressure as recorded during the walking trial was used as a reference to allow the subject to closely reproduce the contact area and pressure distribution as found in the walking trial. Continuous data were collected for 32 seconds at 3-mm

collimation, 3-mm table feed, 210 mAs, and 120 kVp. Data were collected from the plantar surface up to the subject's ankle. Data collection was coordinated and simultaneous data were collected with the SXCT and the F-scan sensor. During the scanning session, no erratic behavior of the F-scan pressure sensor was noted. During the no load scan, data were collected and no extraneous load was recorded due to the x-radiation.

The trial for the subject with DM was conducted as described for the healthy volunteer (above) with the following exceptions: 1) one of the lead reference markers was applied to the sensor at the lateral midfoot instead of the heel to ensure a pressure reading for that marker during forefoot loading in the CT scanner; 2) lead bbs were not affixed to the subject's foot as we did not perform the caliper measurements due to time considerations of the subject.

The raw data from both sessions were transferred to a Siemens satellite CT evaluation console^A and reconstructed at 1-mm slice thickness using the 180_LI ultrahigh algorithm^B. The data were transferred to a Silicon Graphics Indigo2 with Extreme Graphics workstation^C and resampled to 1-mm cubic voxels using AnalyzeTM software^D (37,38).

Data obtained from SXCT and pressure assessment offer the opportunity for almost limitless investigation. For this initial investigation, we focused on a parsimonious number of variables, which the literature and our experience indicate to be most important in predicting plantar pressures. We identified primary variables as arch height (20), soft tissue thickness under the metatarsal heads (19), the angle between the phalanges and the metatarsals (hammer toe deformity: 18), thickness of muscle and thickness of total soft tissue under the midshaft of the metatarsal (relative to loading plate), intrinsic muscle volume, plantar foot pressure, and the contact area of the foot with the loading plate. We measured these variables for the no load and 50 percent loaded conditions in the SXCT scanner for the healthy subject and for the subject with DM and peripheral neuropathy.

The volumetric CT data allow retrospective review of slice data from any perspective. Using a volume rendered image of the foot skeleton, a reference plane was interactively positioned along the midshaft of a metatarsal, and the resulting slice was displayed for measurement of defined variables (**Figure 3**). Volumetric CT measurements

^A Siemens Medical Systems, Inc., Iselin, NJ

^B Software v. 3.42, Tekscan, Boston, MA

^C Silicon Graphics, Inc., Mountain View, CA

Table 1.
Walking trial compared with simulated loading using loading apparatus.

Subj	Condition	Area	Pressure	Location
DM	walking	25.0	886	2 nd met head
DM	50% bw	27.1	753	2 nd met head
Control	walking	53.9	268	3 rd met head
Control	50% bw	49.3	227	3 rd met head

Subj=Subject; Area = control area in cm²; Pressure=peak plantar pressure in kPa; Location=location of peak plantar pressure; DM=person with diabetes mellitus; bw=body weight; met=metatarsal.

were made using the Analyze software system. The arch height, given as the metatarsal angle relative to the floor during stance, was defined by Cavanagh as a significant structural predictor of pressure (20). We measured the metatarsal angle defined by the shaft of a metatarsal relative to a line scribed from the inferior-most part of a metatarsal head to the inferior calcaneus. We measured the angle of the other metatarsals in a similar manner. We used this approach to standardize the measurement, as the angle of the foot to the loading surface was not explicitly controlled during loading.

Soft tissue thickness was measured orthogonal to the loading surface under each metatarsal head. For the first metatarsal, the measurement was made from the sesamoid to the skin surface having the smallest tissue thickness.

Soft tissue thickness under the mid-shaft of each metatarsal was measured to assess the intrinsic muscles of the healthy and diabetic subjects. The length of each metatarsal was measured and the midpoint calculated. The amount of fat and muscle, relative to the plantar skin surface, was measured orthogonal to the metatarsal shaft for each location.

Hammer toe deformity is represented by the angle formed between the metatarsal shaft and the proximal phalanx (18). The reference used for this angular measurement was established using the five tarsometatarsal joint centers, the joint centers of the metatarsals and proximal phalanges, and the joint centers of the middle and distal phalanges. For the great toe, the center of the distal end of the distal phalanx was used. These measurements were made using a volume rendered image of the foot skeleton as a reference and using an oblique cutting plane to define a 2D paraxial image along the shaft of the selected metatarsal and phalanx.

RESULTS

Accuracy of SXCT Data

An initial assessment of spiral CT measurement accuracy was determined on data collected from the healthy subject. Caliper measurements were made between the six lead reference markers and were considered truth. Like measurements were made between pair-wise reference markers from the SXCT data using Analyze software. The mean error between calipers and CT data for the subject with DM was approximately 2 mm, similar to our earlier prosthetics studies (29,39,40). Measurements were made

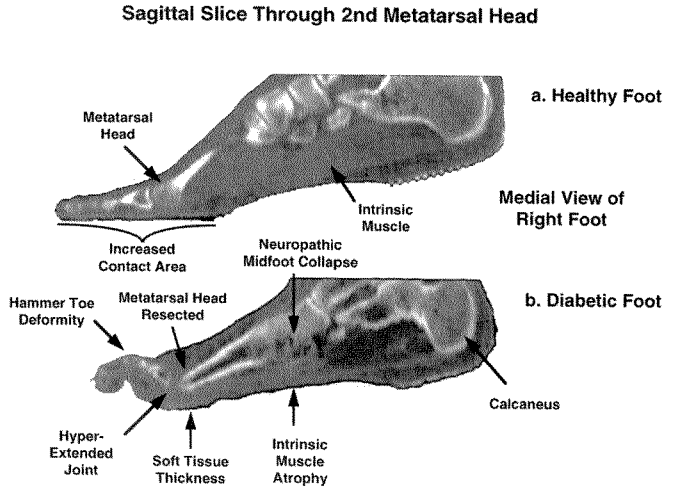


Figure 3. SXCT data along the midshaft of the second metatarsal bones are shown for two volunteers scanned with 50% body weight loads. The healthy subject data (a) had considerably more intrinsic muscle and a larger area of plantar surface contact during loading than the subject with DM (b), who had hammer toe deformity, intrinsic muscle atrophy, and a resected metatarsophalangeal joint, which are all obvious in this sagittal view. The subject with DM presented with an ulcer under his second metatarsal shaft.

^o Biomedical Engineering Resource Unit, Mayo Clinic, MN.

Table 2.

Angle (degrees) of each metatarsal shaft. (Arch height is defined by Met1 angle)

Foot	State	Met 1	Met 2	Met 3	Met 4	Met 5
Control	UW	17.2	22.4	16.1	9.6	2.6
	W	15.8	20.5	17.0	9.0	3.5
DM	UW	9.2	19.4	9.6	2.7	2.8
	W	5.0	13.6	7.2	4.0	-5.8

Met=metatarsal angle in degrees; UW=unweighted; W=weighted; DM=person with diabetes mellitus.

outside of the scanner with an approximation of foot position that would be assumed in the scanner. Previous studies have demonstrated our ability to repeatedly measure lead bbs (precision error less than 1 mm) for similar types of measurements (29,35,41).

Plantar Loading Assessment

Figure 2 shows the plantar pressures during walking (a) and during simulated loading (b) for the person with DM and peripheral neuropathy. Pressure distribution and contact area were very similar in the walking and simulated conditions. **Table 1** shows the contact area (between the forefoot and ground), peak plantar pressure, and location of peak plantar pressure during a walking trial and at 50 percent body weight simulated loading for the subject with DM and peripheral neuropathy and for the healthy subject.

To further test the pressure data, total force was recorded in a sampling of frames and compared with the applied force as monitored by the force scale with digital readout. On average, the forces agreed to within 6.5 percent. Although there are obvious differences between walking and the loaded conditions, these results give us confidence in our ability to simulate contact area and load distribution in the CT scanner compared with walking.

Comparison between Diabetic and Non-diabetic Foot

Examples of results are shown in **Figures 3** and **4**. **Figure 3** shows a sagittal view through the second metatarsal of the healthy subject (**Figure 3a**), and the subject with DM and peripheral neuropathy (**Figure 3b**). Obvious differences include the shape of the metatarsal head, soft tissue thickness (intrinsic muscles) under the shaft of the metatarsal, and amount of hammer toe deformity.

Pressure distribution, contact area, and magnitude are similar for the walking condition compared with the simulated condition. **Figure 4** shows the pressure data superimposed (aligned using the bbs) onto the 3-D image of the foot.

Clearly, the peak pressure is localized over the deformed second metatarsal head.

The angle of the metatarsal shaft was greatest at the second metatarsal head for both subjects and this increased angle corresponded to the highest plantar pressures under the second metatarsal head for each subject. In general, the angle of the metatarsal shaft was less for the subject with DM compared with the healthy control, especially in the weighted conditions (**Table 2**).

We measured the minimum soft-tissue thickness under each metatarsal. These measurements were made using the Analyze software system from sagittal slices. Surprisingly, the soft tissue thickness under the metatarsal head was not less in the subject with DM compared with the healthy subject (**Table 3**).

Hammer toe deformity measurements were recorded for both subjects and are shown in **Figures 3a** and **3b**. The hammer toe deformity is more severe for the patient with DM compared with the healthy subject for the second toe in both the unloaded (57 vs 43°) and loaded (45 vs 25°) conditions (**Table 4**).

Visually, the intrinsic muscle size was strikingly different for the two people. The intrinsic muscles appeared to be essentially nonexistent for the person with DM (**Figure 3**). The soft tissue under the midshaft of the metatarsal was measured according to total soft tissue and by muscle size only. Results are shown in **Figures 3a** and **3b** and **Table 5**,

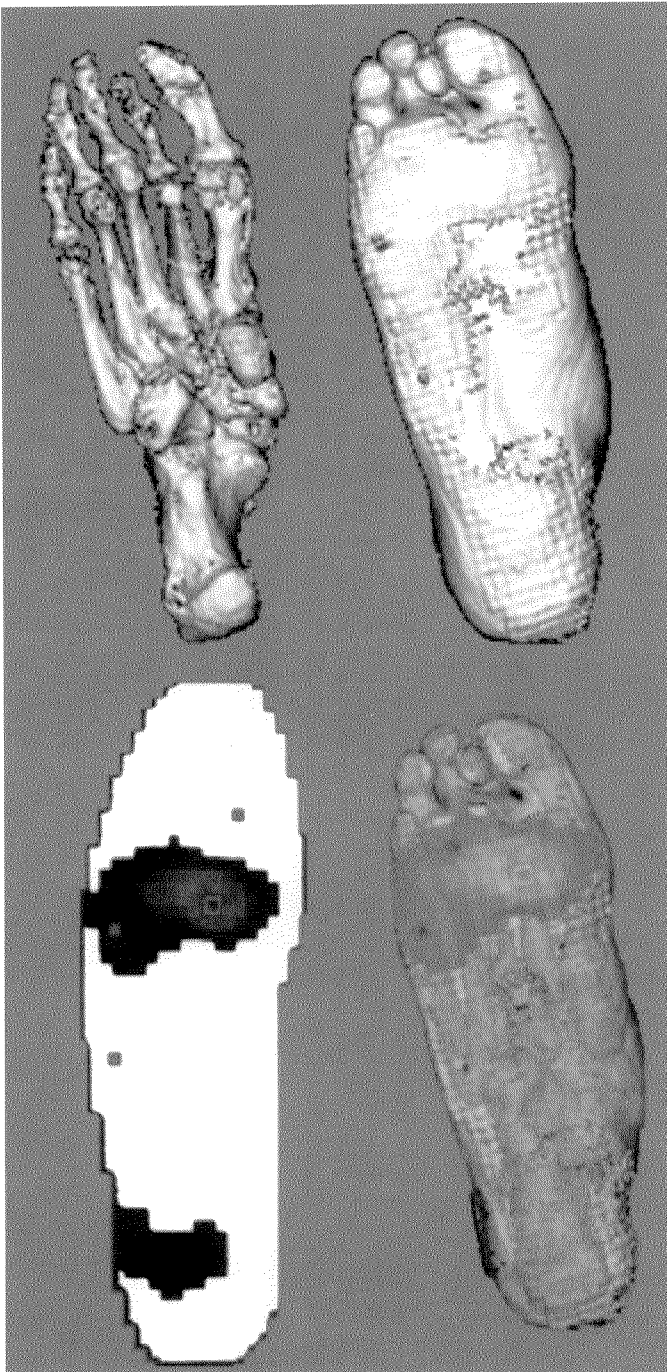


Figure 4.

A subject with DM and peripheral neuropathy and a plantar ulcer was recruited and scanned in the SXCT and pressure assessed with the F-scan pressure sensing system. The F-Scan pressure data (bottom left) were mapped to the SXCT image data using lead BB reference markers, which could be seen in the pressure data and the SXCT data. Peak pressure was seen at the second metatarsal head (bottom right), which was clinically assessed as the site of the ulcer.

and indicate an extreme reduction in soft tissue for the diabetic foot.

DISCUSSION

The results from this investigation suggest that we have similar spiral CT measurement accuracy for the foot as found previously for the residuum, although a statistically significant sample should be evaluated to establish the reliability and accuracy of foot measurements. The precision for these types of measurements has previously been shown to be less than 1 mm for SXCT data of the residuum (29,39,40) and should be similar for the foot. The 2-mm measurement error found for surface marker locations on the subject was most likely due to differences in foot positioning between caliper measurement and CT scanning sessions.

There are no known 3-D studies relating foot structure to plantar pressure with which to compare our results. However, our findings of soft tissue thickness under the metatarsal heads were not consistent with the 2D ultrasonography study by Gooding et al. (19) who showed less soft tissue under the metatarsal heads for people with DM and peripheral neuropathy. In fact, our data showed a greater soft tissue thickness under the second, third, and fourth metatarsal heads. Interestingly, the site of the highest pressure and ulcer (under the second metatarsal head) was also the site having the most soft tissue, which contradicts traditional clinical views regarding the role of soft tissue thickness under the metatarsal heads (19). Palpation of the soft tissue under the metatarsals subjectively indicated the soft tissue of the subject with DM to be stiffer than that of the healthy subject. The stiffer soft tissue transmits more load to the underlying metatarsal heads, which may explain some of the localized stress concentration.

The most severe hammer toe deformity in the subject with DM was seen in the second toe, which corresponds to the ulcer under the second metatarsal head (**Figures 2 and 4**). This is in agreement with Holewski et al. (18) who report that hammer toe deformity had the strongest correlation to ulcer/amputation of all variables studied. During loading, the toes supported little or no load for the subject with DM (leading to a reduced contact area and higher localized pressure) as opposed to the healthy control. Wasting of the intrinsic muscles was also evident in the subject with DM, which is thought to be a cause of hammer toe deformity.

The angle of the second metatarsal was the steepest for both the subjects with and without DM, which also

Table 3.

Soft tissue thickness (mm) under each metatarsal head.

Foot	State	Met 1	Met 2	Met 3	Met 4	Met 5
Control	UW	10.1	8.0	4.5	4.1	6.5
	W	8.5	5.5	4.5	3.5	4.0
DM	UW	9.0	14.0	8.0	7.1	5.0
	W	3.5	7.5	5.0	3.5	2.0

Met=soft tissue under metatarsal head in mm; UW=unweighted; W=weighted; DM=person with diabetes mellitus.

corresponded to peak pressure for both subjects. The subject with DM, however, had a much steeper angle of inclination for the second metatarsal relative to the first and third metatarsal than seen in the healthy control. During plantar loading, the angle of metatarsal inclination for the subject with DM was reduced twice that of the healthy control. The second metatarsal angle also changed more compared with the first and third metatarsal in the subject with DM during loading, which may be related to the increased load at the second metatarsal head.

The reduced angle of metatarsal shafts for the subject with DM compared with the healthy control may be due to the apparent partial collapse of the joints of the midfoot seen in the subject with DM (**Figure 3**). The loss of support from the interosseous ligaments and intrinsic muscles may explain the further reduction in the angle during weighted conditions for the subject with DM.

This study confirmed the clinical assessment for this subject that an orthosis was needed to relieve the pressure under the second metatarsal head and no modifications were made to the orthosis. When the subject was shown the

exceedingly high localized pressure under his second metatarsal head during barefoot walking, however, he began to wear his orthotic shoes at all times and within a few weeks the ulcer was healed.

CONCLUSION

A new method, based on CT imaging and plantar pressure measurement, was developed and implemented for assessment of the diabetic foot. These initial results warrant further study of the relationship between foot structure and pressure. The clinical assumption that reduced soft tissue thickness under the metatarsal heads leads to increased localized pressure and subsequent ulcer was not seen in this preliminary investigation. It is possible that the diabetic subject in this study was not typical. A study including a statistically significant number of subjects and controls should be conducted to establish the relationship of foot structure to plantar pressure. Future studies could utilize these methods to study feet in various stages of gait to reveal possible dynamic changes that may occur.

Table 4.

Angle (degrees) of metatarsal shaft and the proximal phalanx (hammer toe).

Foot	State	M/P1	M/P2	M/P3	M/P4	M/P5
Control	UW	16.2	43.4	45.7	42.5	31.2
	W	15.2	25.4	37.5	36.8	21.7
DM	UW	16.2	57.3	48.2	34.1	21.6
	W	13.0	45.2	35.4	21.8	12.4

M/P = angle between metatarsal/phalanx pair; in degrees; UW=unweighted; W=weighted; DM=person with diabetes mellitus.

Table 5.

Thicknesses (in mm) of soft tissue and muscle under the midshaft of each metatarsal.

Foot	State	Met 1 (mm)		Met 2 (mm)		Met 3 (mm)		Met 4 (mm)		Met 5 (mm)	
		soft	mus								
Healthy	UW	32.6	23.6	38.2	30.4	34.1	26.3	25.1	17.6	20.8	17.2
	W	28.9	18.1	27.8	24.6	29.5	20.5	22.4	14.3	15.5	10.8
DM	UW	25.9	7.1	18.5	6.4	17.1	9.6	14.2	3.2	6.3	2.9
	W	9.7	3.6	14.3	9.1	15.3	12.2	14.9	4.1	6.6	1.0

Met=metatarsal midshaft; soft=soft tissue in mm; mus=muscle in mm; UW=unweighted; W=weighted; DM=person with diabetes mellitus.

Determining the differences between the diabetic and healthy foot, and how these differences relate to plantar pressures, will help clinicians and researchers to understand and manage the structural factors that contribute to skin breakdown.

ACKNOWLEDGMENTS

We wish to acknowledge Ronald Evens, MD and G. James Blaine, PhD, from the Mallinckrodt Institute of Radiology for their support of this project, and Richard Robb and his associates of the Mayo Biomedical Imaging Resource, Rochester, MN, for providing the Analyze software.

REFERENCES

- Reiber GE, Boyko EJ, Smith DG. Lower extremity foot ulcers and amputation in individuals with diabetes. In: Harris MI, Cowie CC, Stern MP, Boyko EJ, et al., editors. *Diabetes in America*, 2nd ed. Washington, DC, US Govt Printing Office (DHSS publ NO. 95-1468); 1995. p. 408–28.
- Pecoraro RE, Reiber GE, Burgess EM. Pathways to diabetic limb amputation: basis for prevention. *Diabetes Care* 1990;13:513–21.
- Most RS, Sinnock P. The epidemiology of lower extremity amputation in diabetic individuals. *Diabetes Care*, 1983;6:87–91.
- American Diabetes Association. *Diabetes: 1993 vital statistics*. Alexandria, VA: American Diabetes Association; 1993. p.26.
- Edmonds ME, Blundell MP, Morris ME, Thomas EM, Cotton LT, Watkins PJ. Improved survival of the diabetic foot: the role of a specialized foot clinic. *Q J Med* 1986;232:763–71.
- Apelqvist J, Ragnarson-Tennvall G, Larsson J, et al. Long term costs for foot ulcers in diabetic patients in a multidisciplinary setting. *Foot Ankle Intl* 1995;16:388–94.
- Boulton AJM, Betts RP, Franks CI, Newrick PG, Ward JD, Duckworth T. Abnormalities of foot pressure in early diabetic neuropathy. *Diabetic Med* 1987;4:225–28.
- Brand PW. The diabetic foot. In: Ellenberg M, Rifkin H, editors. *Diabetes mellitus: theory and practice*, 3rd ed. New Hyde Park, NY: Medical Examination Publishing Co. Inc; 1983. p. 829–49.
- Ctercteko GC, Dhanendran M, Hutton WC, et al. Vertical forces acting on the feet of diabetic patients with neuropathic ulceration. *Br J Surg* 1981;68:608–14.
- Bauman JH, Girling JP, Brand PW. Plantar pressures and trophic ulceration: an evaluation of footwear. *J Bone Joint Surg* 1963;45(B):652–73.
- Lord M, Hosein R. Pressure redistribution by molded inserts in diabetic footwear: a pilot study. *J Rehabil Res Dev* 1994; 31:214–21.
- Mueller MJ, Strube MJ. Therapeutic footwear: enhanced function in people with diabetes and transmetatarsal amputation. *Arch Phys Med Rehabil* 1997;78:952–6.
- Mueller MJ, Strube MJ, Allen BT. Therapeutic footwear can reduce plantar pressures in patients with diabetes and transmetatarsal amputation. *Diabetes Care* 1997;20:637–41.
- Nawoczinski DA, Birke JA, Coleman WC. Effect of rocker sole design on plantar forefoot pressures. *J AM Podiatr Med Assoc* 1988;78:455–60.
- Schaff PS, Cavanagh PR. Shoes for the insensitive foot: the effect of a “rocker bottom” shoe modification on plantar pressure distribution. *Foot Ankle* 1990;11:129–49.
- Mueller MJ, Diamond JE, Sinacore DR, et al. Total contact casting in treatment of diabetic plantar ulcers: controlled clinical trial. *Diabetes Care* 1989; 12:384–8.
- Sinacore DR. Total contact casting for diabetic neuropathic ulcers. *Phys Ther* 1996;76:296–301.
- Holewski JJ, Moss KM, Stess RM, Graf PM, Grunfeld C. Prevalence of foot pathology and lower extremity complications in a diabetic outpatient clinic. *J Rehabil Res Dev* 1989;26:35–44.
- Gooding GAW, Stess RM, Graf PM, Moss KM, Louie KS, Grunfeld C. Sonography of the sole of the foot: evidence for loss of foot pad thickness and its relationship to ulceration of the foot. *Investigat Radiol* 1986;21:45–8.
- Cavanagh PR, Morag E, Boulton AJM, Young MJ, Deffner KT, Pammer SE. The relationship of static foot structure to dynamic foot function. *J Biomechan* 1997;30:243–50.
- Mueller MJ, Minor SD, Diamond JE, Blair VP. Relationship of

- foot deformity to ulcer location in patients with diabetes mellitus. *Phys Ther* 1990;70:356-62.
22. Fishman EK, Wyatt SH, Bluemke DA, Urban BA. Spiral CT of musculoskeletal pathology: preliminary observations. *Skeletal Radiol* 1993;22(4):253-6.
 23. Kalender WA, Polacin A. Physical performance characteristics of spiral CT scanning. *Med Phys* 1991;18(5):910-5.
 24. Kalender WA, Polacin A. A comparison of conventional and spiral CT: An experimental study on the detection of spherical lesions. *J Comput Assist Tomogr* 1994;18(2):167-76.
 25. Kalender WA, Seissler W, Klotz E, Vock P. Spiral volumetric CT with single-breath-hold technique, continuous transport, and continuous scanner rotation. *Radiology* 1990;176:181-3.
 26. Heiken JP, Brink JA, Vannier MW. Spiral (helical) CT (Review). *Radiology* 1993;189(3):647-56.
 27. Wang G, Vannier MW. Longitudinal resolution in volumetric x-ray computerized tomography: Analytical comparison between conventional and helical computerized tomography. *Med Phys* 1994;21(3):429-33.
 28. Brink JA, Heiken JP, Wang G, McEneaney KW, Schlueter FJ, Vannier MW. Helical CT: principles and technical considerations. *Radiographics* 1994;14(4):887-93.
 29. Commean PK, Smith KE, Cheverud JM, Vannier MW. Precision of surface measurements for below-knee residua. *Arch Phys Med Rehabil* 1996;77(5):477-86.
 30. Commean PK, Smith KE, Vannier MW. Lower extremity residual limb slippage within the prosthesis. *Arch Phys Med Rehabil* 1997;78(5):476-85.
 31. Smith KE, Commean PK, Bhatia G, Vannier MW. Validation of spiral CT and optical surface scanning for use in lower limb remnant volumetry. *Prosthet Orthot Intl* 1995;19:97-107.
 32. Smith KE, Commean PK, Vannier MW. Residual-limb shape change: Three-dimensional CT scan measurement and depiction in vivo. *Radiology* 1996;200(3):843-50.
 33. Smith KE, Vannier MW, Commean PK. Spiral CT volumetry of below knee residua. *IEEE Trans Rehabil Eng* 1995;3(3):235-41.
 34. Vannier MW, Commean PK, Brundsdon BS, Smith KE. Visualization of socket fit in lower limb amputees by volumetric CT scanning. *IEEE Comput Graph Eng* 1997;17(5):16-29.
 35. Vannier MW, Commean PK, Smith KE. Three-dimensional lower-extremity residua measurement systems error analysis. *J Prosthet Orthot* 1997;9(2):67-76.
 36. Mueller MJ, Strube MJ. Generalizability of in-shoe peak pressure measures using the F-scan system. *Clin Biomech* 1996;11:159-64.
 37. Robb RA. Three-dimensional biomedical imaging: principles and practice. New York: VCH Publishers, Inc.; 1995.
 38. Robb RA, Barillot C. Interactive display and analysis of 3-D medical images. *IEEE Trans Med Imaging* 1989;8(3):217-26.
 39. Commean PK, Smith KE, Bhatia G, Vannier MW. Validation of spiral computed tomography and optical surface scanning for 3-D limb prosthesis design. Proceedings of the IMAGE VII Conference, Image Society, Tucson, AZ; 1994. p. 369-81.
 40. Commean PK, Smith KE, Vannier MW, Hildebolt C, Pilgram T. Precision and accuracy of 3-D lower extremity residua measurement systems. *SPIE Med Imaging* 1996;2710:494-510.
 41. Kohn LAP, Cheverud JM, Bhatia G, Commean PK, Smith KE, Vannier MW. Anthropometric optical surface imaging system repeatability, precision, and validation. *Ann Plastic Surg* 1995;34:362-71.

Submitted for publication June 22, 1998. Accepted August 11, 1998.